

*XVII IMEKO World Congress  
Metrology in the 3rd Millennium  
June 22–27, 2003, Dubrovnik, Croatia*

## HMSM PHOTODETECTORS FOR HIGH-SPEED APPLICATIONS

*Andrea Cataldo\**, *Bahram Nabet<sup>§</sup>*, *Adriano Cola<sup>°</sup>*, *Amerigo Trotta\**.

\* Dip.to Ingegneria dell'Innovazione, University of Lecce, Lecce, Italy; <sup>§</sup> Electrical and Computer Engineering Dept., Drexel University, Philadelphia, USA; <sup>°</sup> CNR-IMM, sezione di Lecce, Lecce, Italy.

**Abstract** - In this paper we describe the characterization of a family of optical devices based on heterojunction and heterodimensional structures and we investigate their static and dynamic properties. Such devices are good candidates, due to their high performance, for utilization as the sensing element for the realization of sensors in the fields of telecommunications, remote sensing, LIDAR and medical imaging. First, we present a Heterostructure Metal-Semiconductor-Metal (HMSM) photodetectors that employ a uniformly doped GaAs/AlGaAs heterojunction for the dual purpose of barrier height enhancement and creating an internal electric field that aids in the transport and collection of the photogenerated electrons. In this first family of devices, two doping levels are compared showing the direct effect of the aiding field due to modulation doping. Subsequently, we analyse a novel Resonant-Cavity-Enhanced (RCE) HMSM photodetector in which a Distributed Bragg Reflector (DBR) is employed in order to reduce the thickness of the absorption layer thus achieving good responsivity and high speed as well as wavelength selectivity. Current-voltage, photocurrent spectra and high-speed time response measurements point out the better performance of this last family of detectors, as they can operate in tens of Giga-Hertz range with low dark current and high responsivity. Particularly, the I-V curves show a very low dark current (around 10 picoamps at operative biases) and the photocurrent spectrum shows a clear peak at 850 nm wavelength. Combination of very low dark current wavelength selectivity, and compatibility with high electron mobility transistors makes these devices especially suitable for the above-mentioned applications.

**Keywords:** Heterostructure Metal-Semiconductor-Metal, Two-Dimensional Electron Gas, Resonant-Cavity-Enhanced.

### 1. INTRODUCTION

This article discusses two classes of high-speed, low-noise photodetectors, at near-infrared wavelength, both based on AlGaAs/GaAs heterojunctions. First, we describe a device in which modulation doping of a heterojunction produces an internal field that aids in the transport and collection of carriers. Second, in order to improve on the speed of response by reducing transit length of the carrier, a Resonant Cavity Enhanced (RCE) photodetector is presented, which can provide high quantum-efficiency

detection as well as wavelength selectivity [6] [7]. A schematic cross-section of a device structure based on AlGaAs/GaAs heterojunction is shown in Figure 1.

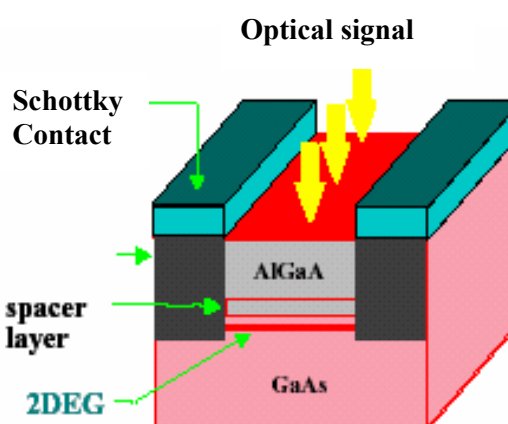


Fig.1. Schematic cross-section of a device structure based on AlGaAs/GaAs heterojunction.

The basic properties of these devices are changed by the presence of a two-dimensional electron gas (2-DEG) that is formed at the interface of the heterojunction and contacted with Schottky metal electrodes. This 2DEG improves the current transport behaviour under both dark and light conditions [1]. Furthermore, these devices have the same structures of the High Electron Mobility Transistor (HEMT), but with the crucial distinction that the Schottky contacts are made parallel to the heterojunction hence in the lateral plane these devices are similar to a Metal-Semiconductor-Metal (MSM) photodetector. In this case current conduction is due dominantly to thermionic emission and under reverse bias the direction of current is from metal to semiconductor [2] [4] [5].

In addition, we have realized on the same device structure a vertical RCE in order to enhance the detection performance in terms of quantum efficiency –high speed trade off. Resonant cavity technique offers the possibility to balance such conflict between fast speed and sensitivity [3]. We report a comprehensive study of the electrical behaviour of these devices under bias. Current-Voltage measurements confirm the 2-DEG role in aiding photocarriers transport and in reducing dark current due to the barrier enhancement,

while photocurrent measurement showed good optical response around 850 nm .

## 2. STATIC CHARACTERIZATION OF THE DEVICES

With reference to the devices with uniform doping levels of the AlGaAs layer, current-voltage characteristics under dark were measured. The I-V curves for two different doping levels of the AlGaAs, are shown in Figure 2, in dark and under a 670 nm laser illumination. We observe: dark current levels in the tens of picoamps, a large dynamic range due to very low noise levels, that is, more than 5 order of magnitude change that is observed for about 0.2 mW of optical power, lower dark current and larger photoresponse for higher doping level of AlGaAs.

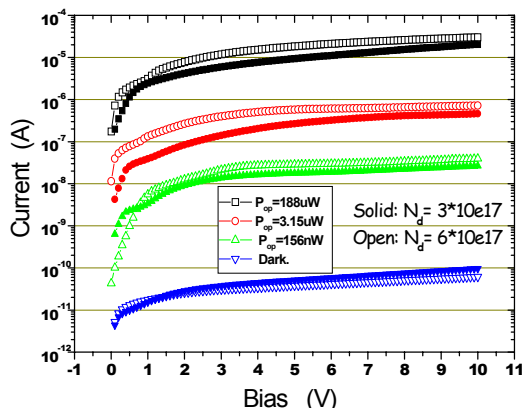


Fig. 2. I-V measurements under dark and illumination for two different uniform doping levels.

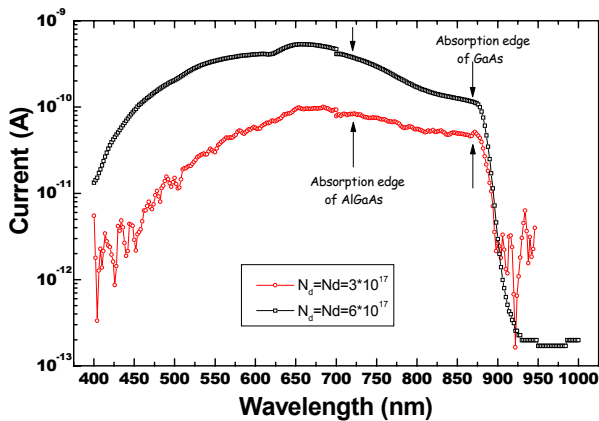


Fig. 3. Photocurrent spectra for two different uniform doping levels.

The spectral response of the low and high-doping samples, in the range of 400-1000 nm, is shown in Figure 3.

The signal was measured by a lock-in amplifier and the spectral response was measured under 10 V reverse bias. It is interesting to note that, in the region where only GaAs absorbs, as the wavelength decreases, the high-doping sample increases the collection of photo-generated carriers with respect to the low-doping. This result, in conjunction of the data of Figure 1, is consistent with the aiding role of the vertical electric field, which is stronger in the case of higher doping.

Similar measurements were performed on the RCE based devices; Figure 4 shows I-V curves under dark and under dc light excitation at two different optical powers for the devices with and without  $\delta$ -doping. Under dark, the doped sample shows a soft increase of the current with voltage, with values, at 20 V, lower than 30 pA. The behaviour of the undoped sample is rather different, as the current strongly increases at low voltage (2-3 V) up to about 30 pA. It is worthwhile to note that the lower values for current of the doped sample are in qualitative agreement with the effect of the repulsion between the electrons in the metal contact and the electrons in the 2DEG; similar to the photodetectors with uniform doping, above.

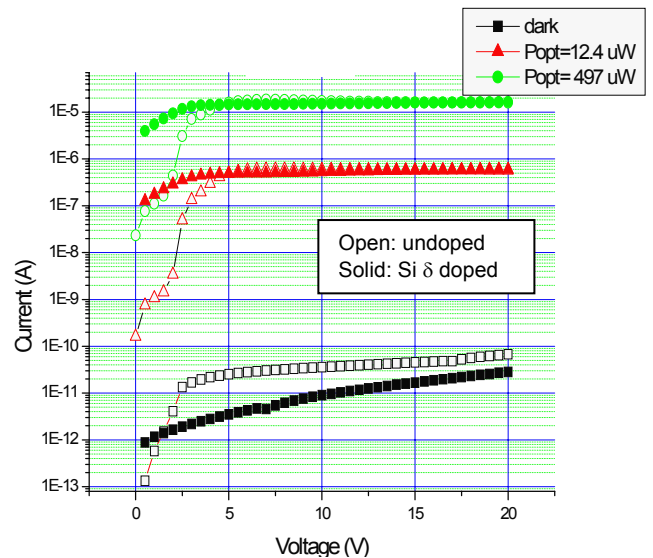


Fig. 4. Comparison of I-V behaviour between the delta-doped and undoped devices with RCE.

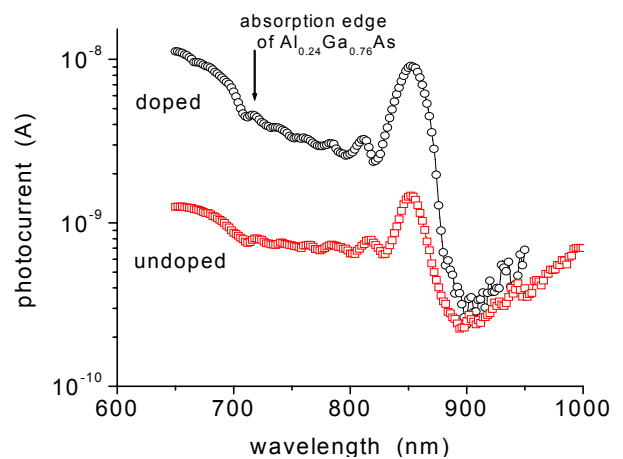


Fig. 5. Photocurrent spectral response for undoped and delta-doped devices with RCE.

The light response has been measured by using a 850nm pigtailed laser, with the optical fiber of 9 $\mu$ m core positioned just in proximity, but not perpendicularly, of the active area of the device. Due to the very low leakage current and to the

good responsivity, both detectors show a large dynamic response, the undoped samples showing lower photocurrent values at low voltage. However, for  $V > 2-3V$ , the photocurrent curves of both samples merge and strongly saturate. Saturation indicates that complete collection of the photo-generated carriers occurs.

Figure 5 illustrates the experimental photocurrent spectral response of the doped and undoped RCE-HMSM photodetectors. The resonant peak is around 850 nm and the FWHM value is 30 nm. An increase of photocurrent is observed around 710 nm, which is due to absorption in AlGaAs layers. We note that the spectral response is, at all the wavelengths, much higher for the doped than for the undoped device. This is consistent with the photocurrent response to the monochromatic laser at 850nm, by taking into account that in Figure 5 the light intensity is pretty low and the applied voltage is 10V. Some photocurrent oscillations are evident between 720nm and 850nm in both devices which can be attributed to the effect of the Bragg reflector.

### 3. DYNAMIC CHARACTERIZATION OF THE DEVICES

High-speed time measurements were made using a mode-locked Ti: Sapphire laser, in order to excite picosecond pulses in the devices. The laser provided ~ 100fs wide optical pulses with 850nm wavelength and 76 MHz repetition rate. We have used an average optical power of 0.1 mW which corresponds to a pulse energy of about 1.4pJ. The optical pulses impinge on the photodiodes biased through a bias tee. The photodiode RF signal is measured on-wafer with a Tektronix 11801C digital sampling oscilloscope.

The effect of aiding field, introduced through the 2DEG, was also observed in time response characterization performed on both families of devices.

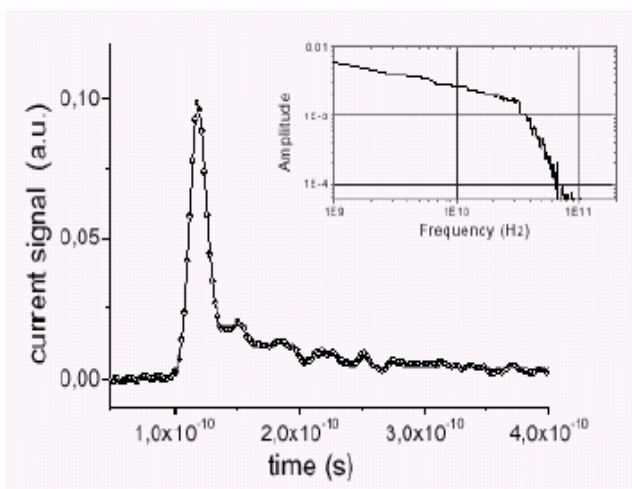


Fig. 6. Temporal response of a  $W = 2 \mu\text{m}$   $G = \mu\text{m}$  uniform doped device, inset shows the calculated frequency response.

Figure 6 reports a typical trace for a uniform doping device with interdigital contact finger width  $W = 2 \mu\text{m}$  and inter-finger distance  $G = 2 \mu\text{m}$ , which shows a short (less than 10 ps long) peak with short full width at half max (FWHM) that is followed by a long tail of low amplitude. The inset of the same figure also reports the calculated FFT of the data indicating a sharp drop in amplitude after 30 GHz. Table I summarizes the results: for each contact geometry, the peak amplitude and the width of the peak are reported.

TABLE I. Comparison of peak amplitude and width of response for different interdigital structures for two uniform doping levels.

Contact Width, Gap ( $\mu\text{m}$ )	Amplitude Low-doping (a.u.)	Amplitude high-doping (a.u.)	Width Low-doping (ps)	Width high-doping (ps)
1,2	0.218	0.239	8.68	7.74
2,2	0.262	0.364	8.79	7.74
1,4	0.185	0.216	8.23	7.31
2,4	0.157	0.218	9.26	8.15

The amplitude of the peaks is systematically higher for the high-doping sample and, interestingly, the width of the peak shows a slight decrease thus indicating a faster response. The results show also that the gap affects greatly the peak amplitude, the sample with  $G = 2 \mu\text{m}$  having higher amplitude that the corresponding with  $G = 4 \mu\text{m}$ . This is explained in terms of reduction of transit time as well as less effective trapping due to decrease in the distance between contacts.

Figure 7 shows the temporal response of a delta-doped photodetector with the RCE for a geometry  $W = 1 \mu\text{m}$  and  $G = 4 \mu\text{m}$ , measured at 20 V bias. From the figure, FWHM of the time response is 8,1 ps, its rise time is 8,8 ps, and fall time is 9 ps. Fast Fourier Transform of the data is shown in the inset of figure and has a 3 dB bandwidth of 34 GHz. The fact that rise time, fall time and FWHM of the peak are all comparable, suggests that the electrical circuit limits the speed of response as measured by the oscilloscope.

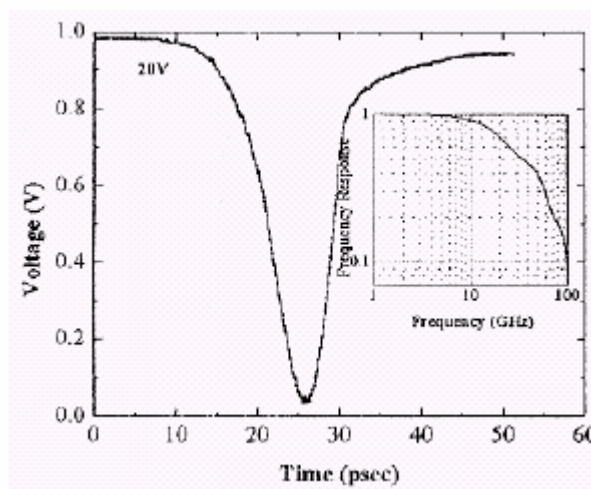


Fig. 7. Temporal response of a  $W = 1 \mu\text{m}$   $G = 4 \mu\text{m}$  delta doped device with RCE, inset shows the calculated frequency response.

In order to check the reliability of the measurements, we have carried out measurements over all the devices of different contact geometry, both delta-doped and undoped. The results are summarized in Table II which reports, for all the investigated samples, the amplitude and FWHM of the peak, obtained at 20 V bias. The peak amplitude has been properly normalized to take into account the active area of the device. The results are consistent with the previous case, showing that, the doped samples have peak amplitude always greater than the undoped samples. This result, which refers to the dynamic response, confirms the photocurrent measurements carried out under static conditions. The samples with  $G = 2 \mu\text{m}$  have peak amplitude always greater than those with  $G = 4 \mu\text{m}$ , for each  $W$ . This is indicative of incomplete collection of charge, probably due to trapping processes. The pulse widths of the undoped samples of different  $W$  and  $G$  are comparable among them; the same holds for the doped samples (except one). Moreover, the doped samples have peak widths shorter than undoped samples. Even in this case, doped samples show better performance than the undoped ones since the shorter pulse width means a higher detector bandwidth. It is quite surprising that the detectors showing higher responsivity also show faster response, as the two figures of merit are usually in contradiction.

TABLE II. Peak amplitudes and widths of temporal response of the delta-doped and undoped devices with RCE, biased at 20V, for different interdigital structures.

Contact Width, Gap ( $\mu\text{m}$ )	Amplitude delta-doped (a.u.)	Amplitude undoped (a.u.)	Width delta-doped (ps)	Width undoped (ps)
1,2	0.331	0.192	7.97	9.45
2,2	0.252	0.103	7.03	10.16
1,4	0.292	0.207	11.9	10.38
2,4	0.206	0.111	7.11	12.04

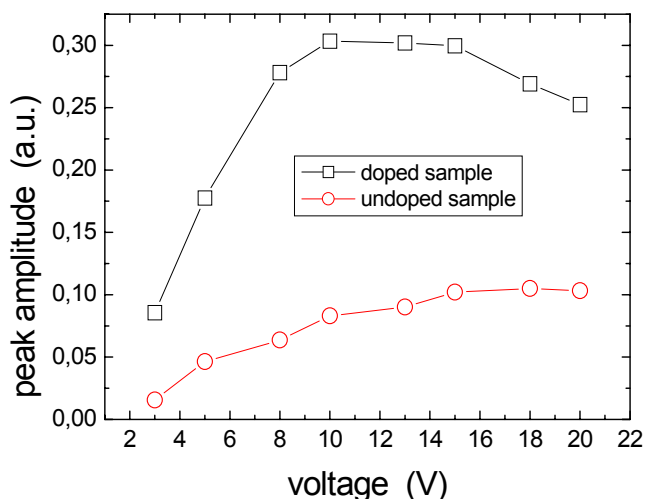


Fig.8. Peak amplitudes as function of the applied voltage, for the delta-doped and undoped samples with  $W=1, G=4$ .

In Figure 8 we report the peak amplitude of the induced pulses as a function of the applied voltage. The doped

sample shows a steep increase of the amplitude, then a saturation around 10 V and finally, for  $V > 15$  V a slight decrease. The undoped sample shows lower values which tend toward saturation around 18 V.

#### 4. CONCLUSIONS

We have reported a comprehensive characterization of a family of photodetectors that use a doped heterojunction to enhance the Schottky barrier and, more importantly, create an internal electric field that aids in the transport and collection of electrons. First, devices were compared when the only variant was the doping level thus showing the effect of this internal aiding field. Current-voltage data shows the low dark current and high dynamic range of the device. Photocurrent spectra comparing the two devices show a marked increase at all wavelengths for the high doped device. In addition, we have characterized a HMSM Schottky photodetector, and have demonstrated the performance improvement due to a resonant-cavity that includes narrow spectral bandwidth. These results indicates that the presence of a delta-doped sheet in the upper AlGaAs layer, plays an important role, in terms of barrier enhancement and internal electric field aiding in the transport of photocarriers. These devices thus exhibit very low dark current wavelength selectivity, and sensitivity. High speed time response data indicates that the devices easily operate in tens of Gigahertz with the doped devices showing much higher peak of response with no adverse effect, even slight improvement, of rise time and FWHM. Based on this comprehensive evaluation, we suggest that these heterojunction based devices are excellent candidates for high-speed optical communication applications.

#### REFERENCES

- [1] B. Nabet, "A Heterojunction Metal-Semiconductor-Metal Photodetector", IEEE Photonics Techno. Lett., vol.9, no.2, pp.223-225, Feb.1997.
- [2] A. Anwar, and B. Nabet, "Barrier Enhancement Mechanisms in Heterodimensional Contacts and their Effect of Current Transport", Trans.On Microwave Theory and Techniques, January 2002.
- [3] M.S. Unlu, and S. Strite, "Resonant Cavity Enhanced Photonic Devices" J. Appl. Phys., vol.78, no.2, pp. 607-639, July 1995.
- [4] B. Nabet, A. Cola, F. Quaranta, and M. Cesareo, R. Rossi, and R. Fucci, and A. Anwar, "Electron Cloud Effect on Current Injection Across a Schottky Contact", Appl. Phys. Lett., vol. 77, no. 24, pp. 4007-4009, Dec. 2001.
- [5] J.B.D. Soole, and H. Schumacher, "Transit-Time Limited Frequency Response of InGaAs MSM Photodetectors", IEEE Trans. Electron Devices, vol. 37, no. 11, pp. 2285-91, 1990.
- [6] S. Adachi, "GaAs, AlAs, and AlxGa1-xAs: Material parameters for use in research and device applications", J. Appl. Phys., vol.58, no.3, pp.R1-R29, August 1985.
- [7] X.Chen, B. Nabet, F. Quaranta, A. Cola, and M. Currie "A Resonant-Cavity-Enhanced Heterostructure Metal-Semiconductor-Metal Photodetector" Appl. Phys. Lett., vol. 80, pag. 3222, (2002).

---

**Authors:** - Dr. Andrea Cataldo, Dept. Ingegneria Innovazione, University of Lecce, via Monteroni, 73100, Lecce, Italy, phone: +39 0832 320207, e-mail: [andrea.cataldo@unile.it](mailto:andrea.cataldo@unile.it)

- Professor Bahram Nabet, Electrical and Computer Engineering Dept., Drexel University, 19104, Philadelphia, PA, USA, phone: 001 215 895 6761, e-mail: [nabet@cbis.ece.drexel.edu](mailto:nabet@cbis.ece.drexel.edu)

- Dr. Adriano Cola, CNR-IMM Sez. Lecce, via Monteroni, 73100, Lecce, Italy, phone: +39 0832 320243, e-mail: [adriano.cola@imm.cnr.it](mailto:adriano.cola@imm.cnr.it)

- Professor Amerigo Trotta, Dept. Ingegneria Innovazione, University of Lecce, via Monteroni, 73100, Lecce, Italy, phone: +39 0832 320207, e-mail: [amerigo.trotta@unile.it](mailto:amerigo.trotta@unile.it)